Application of mode-coupling theory to solvation dynamics

Jangseok Ma, David Vanden Bout,* and Mark Berg
Department of Chemistry and Biochemistry, University of South Carolina, Columbia, South Carolina 29208†
(Received 4 April 1996)

Mode-coupling theory (MCT) is applied to the dynamics of electronic-state solvation. Solvation dynamics in two solvents, propylene carbonate and *n*-butylbenzene, are analyzed by both mode-coupling theory and more standard empirical methods. Fits of the solvation response function allow all the MCT parameters to be extracted. In both liquids, the α and β regions overlap strongly and a simultaneous fit of both regions is required. In the case of propylene carbonate, both β- and α-relaxation components are clearly present. The crossover temperature T_c and exponent parameter λ agree with those found by the light-scattering experiments of Du *et al.* [Phys. Rev. E **49**, 2192 (1994)], showing that these parameters are independent of experiment, as predicted by MCT. In *n*-butylbenzene, both a standard fit without β relaxation and a MCT fit including β relaxation agree well with the data. The value of T_c found disagrees with the value found by the impulsive stimulated thermal scattering experiments of Yang, Muller, and Nelson. In both liquids, the fits extend well above the melting points into the low-viscosity, normal liquid range. [S1063-651X(96)09709-7]

PACS number(s): 64.70.Pf, 61.20.Lc, 78.47.+p, 33.15.Vb

I. INTRODUCTION

This paper brings together two active areas of research on the dynamics of liquids: the dynamics of electronic-state solvation and mode-coupling theories of supercooled liquids. Solvation experiments examine how the electronic states of a solute molecule are perturbed by the motion of the surrounding solvent molecules [1–4]. The equilibrated solute molecules are electronically excited by a short pulse of light. As a result of the excitation, the interaction potential of the solute with the solvent is changed, and the solvent reorganizes in response to the new forces. The dynamics of the solvent are followed in time by measuring the shift in the electronic transition as the relaxation proceeds. The results have profound consequences for the rates of chemical reaction in solution, and especially for electron transfer reactions. In the last several years, new theoretical approaches have appeared [5–10], standard experiments have improved their time resolution [11–13], and echo experiments have provided a new approach to solvation dynamics [14–21].

During the same period, there has also been a dramatic advance in the use of mode-coupling theories (MCTs), to explain the dynamics of supercooled liquids [22–27]. These theories are schematic in the sense that they examine equations that have features typical of all liquids, but do not attempt to model any one specific system. Nonetheless, the MCT makes a variety of quantitative predictions about the shapes of relaxation functions, the form of the temperature dependence of the relaxation times, and the relationship between these two features.

Although solvation experiments have been reported in supercooled liquids [28–38], MCT has never been used to analyze them. We have recently used transient hole burning to measure the solvation response functions in two supercooled systems: *s*-tetrazine in propylene carbonate [33] and dimethyl-*s*-tetrazine in *n*-butylbenzene [34,35]. Both solvents are fragile glass formers, the type of liquid that MCT is intended for. The solvation data are in the picosecond to nanosecond time range, where many of the characteristic features of MCT should be observed. Although testing MCTs was not envisioned when these data were collected, we will show that MCT can be successfully applied to them.

In the last several years, there have been numerous experiments that test various aspects of MCT. Almost all these tests have relied on either light-scattering [39–56] or neutron-scattering [54–70] measurements. However, one of the most powerful predictions of MCT is that any dynamical experiment should yield the same values of certain parameters. In particular, the crossover temperature T_c and the critical exponent λ, as well as the various exponents derived from λ, should transfer between experiments. Transferability of MCT results between neutron- and light-scattering experiments has been demonstrated in the case of $CaKNO_3$ [46–56].

Solvation experiments offer a distinctly different measure of dynamics with which to test MCT predictions. In solvation experiments, the solute molecule can be viewed as a molecular size transducer, which both creates a perturbing field and also measures the response to the field. Thus, the solvation measurement examines short-range dynamics, whereas light-scattering methods inherently look at long-wavelength dynamics. Neutron scattering measures dynamics on a molecular length scale, but measures the response to a different perturbing field than that created by changing a solute's electronic state (see Sec. II A for more discussion).

This paper will show that both the α- and β-scaling regions predicted by MCT are found in solvation response functions. Moreover, the temperature dependence of the corresponding time constants τ_α and τ_β follow the power-law forms given by MCT. For propylene carbonate, there are also

*Present address: Dept. of Chemistry, University of Minnesota, Minneapolis, MN 55418.
†FAX: (803) 777-9521; electronic address: berg@psc.sc.edu

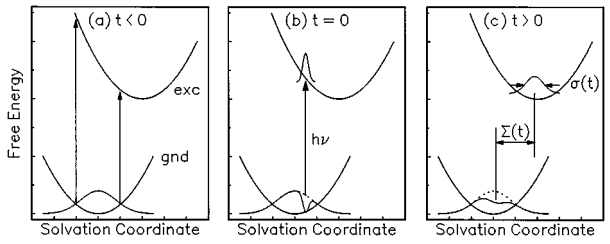

FIG. 1. Schematic of the transient hole burning experiment. (a) Due to the shift in the potential curves for the ground and excited states, different positions within the equilibrium distribution in the ground state have different absorption frequencies. (b) A subpicosecond pulse of light excites only molecules at a particular solvation coordinate. (c) Motion of the solvent causes both the ground-state hole and the excited-state antihole to evolve in time. The solvation dynamics are monitored by either the increase in Stokes shift $\Sigma(t)$ or the hole width $\sigma(t)$ as measured in a time-resolved transmission spectrum.

MCT analyses of both light scattering [42,52,55] and neutron scattering [55,59]. The MCT fits to our solvation data in propylene carbonate yield the same T_c and λ found from light scattering. For *n*-butylbenzene there is a recent MCT analysis of impulsive stimulated thermal scattering (ISTS) experiments, a time-domain equivalent of depolarized light scattering [39]. In this case, the solvation and ISTS experiments arrive at values of T_c that differ by 10 K. This difference is larger than expected.

Not only do solvation data provide a valuable test of MCT, MCT also has significant implications for interpreting solvation dynamics. Complex nonexponential shapes are often found for solvation response functions. We will show that β relaxation is clearly important in propylene carbonate and can explain the temperature-dependent form of the relaxation. β relaxation may be important in *n*-butylbenzene as well. Furthermore, the MCT relations not only apply to the supercooled region with long relaxation times, but remain valid for temperatures well above the melting points and for relaxation times in the picosecond range.

In addition to the MCT analysis of the data, we also include a more standard, empirical analysis for comparison. This comparison is important, given the amount of dynamical data that has been successfully analyzed by standard methods. In propylene carbonate, MCT clearly gives a better fit to the data than standard methods. In *n*-butylbenzene, the standard and MCT analyses are equally good, although the interpretations of the data are quite different. Thus the success of standard treatments does not preclude the applicability of MCT.

II. BACKGROUND

A. The transient hole burning experiment

Detailed descriptions of the theory and implementation of the transient hole burning experiment have been published previously [34–38]. Figure 1 helps to discuss the basic principles. The energy of both the ground and excited electronic states of the solute are plotted as functions of the solvation coordinate, whose exact form depends on the nature of the solvent-solute interaction. Due to the disorder of the solvent, the solute molecules will be in a variety of local environments distributed about the minimum energy value of the solvent coordinate [Fig. 1(a)]. In the excited state, the minimum of the potential curve is shifted to a different value of the solvent coordinate. As a result, the transition energy varies with solvent coordinate: high on the left-hand side of Fig. 1(a), and low on the right-hand side.

In the transient hole burning experiment, a subpicosecond pulse of light excites only those solute molecules with a particular value of the solvent coordinate [Fig. 1(b)]. This leaves a ''hole'' in the ground-state distribution and a narrow ''antihole'' in the excited state. These nonequilibrium distributions evolve with time [Fig. 1(c)]. The ground-state hole shifts toward the ground-state minimum and broadens. The excited-state antihole shifts toward the excited-state minimum and also broadens. Both features are measured as a function of time after excitation by measuring the transmission spectrum of the sample. The solvation dynamics can be derived either from the time dependence of the hole or antihole widths $\sigma(t)$, or from the Stokes shift $\Sigma(t)$, i.e., the frequency splitting between the ground-state hole and the excited-state antihole [37]. All measurements discussed in this paper are based on Stokes shifts. The response function for the solvation coordinate is easily derived from these measurements [34–37]. Because the initial value of the Stokes shift is known to be zero, the absolute value of the response function is known, even if a portion of the dynamics is faster than the time resolution of the experiment. In *n*-butylbenzene, a related time-resolved fluorescence technique [1–4] was used to extend the measurements to longer times [34].

The nature of the solvent-solute interaction and the solvation coordinate are still being debated [7,10,13,33]. In some systems, charge rearrangement in the excited state changes the local electric field after excitation [1–4]. The solvent response is primarily reorientation of solvent dipoles, and the solvation coordinate is a collective reorientation coordinate. In this case, the solvation experiment resembles a large *k*-vector dielectric relaxation experiment. In other systems, a change in size of the solute upon excitation appears to be the dominant interaction mechanism [7]. The solvent coordinate is the radius of the cavity containing the solute, and the dynamics are related to shear relaxation. The solvation experiment then resembles a large *k*-vector ultrasound measurement. The latter mechanism appears to dominate for dimethyl-*s*-tetrazine in *n*-butylbenzene [7], but the mechanism is still uncertain for *s*-tetrazine in propylene carbonate [33]. Fortunately, this uncertainty is not a problem, because the predictions of MCT are independent of the nature of the perturbing field used.

B. Standard analysis of dynamics

The standard treatment of the dynamics of relaxation in supercooled liquids contains three major features [71]. First, the response functions have a nonexponential shape that is described by a stretched exponential

$$R_e(t) = A \exp\left[-\left(\frac{t}{\tau_e}\right)^{\beta_e}\right]. \tag{1}$$

(The very similar Cole-Davidson function is often used for frequency domain experiments [72].) Second, the time-temperature superposition principle holds that the shape of $R(t)$ is independent of temperature. In the case of the stretched exponential, this principle implies that β_e is a constant with changing temperature. Finally, the dependence of τ_e on temperature T is given by the Vogel-Fulcher formula

$$\langle \tau_e \rangle = \frac{\Gamma(\beta_e^{-1})}{\beta_e}\ \tau_e = \tau_e^0\ \exp\left(\frac{DT_0}{T-T_0}\right), \tag{2}$$

where T_0 is a temperature slightly below the laboratory glass transition temperature T_g.

Justifications for these results have been proposed, but none has reached general consensus as a complete explanation [71]. This scheme must be taken as largely empirical. Deviations from this scheme have often been noted, and other formulations have been proposed. However, this treatment has been widely applied with reasonable success, and is an important reference point for judging the effectiveness of MCT in fitting experimental data.

C. Mode-coupling theory

Excellent reviews of both the theoretical development of MCT and its comparison to experiment are available [22–27]. We will summarize only the features that are important in analyzing our data.

In dense liquid systems, the dynamics initially divide into two regions. The fastest component, in the range of a few hundred femtoseconds, has been called inertial, phononlike, or instantaneous normal-mode motion in the solvation literature, and is referred to as microscopic motion in the mode-coupling literature. The slower components are described as diffusive, structural, or collective motions. Aside from the difference in time scale, the phonon motion is characterized by a weak temperature dependence, whereas the structural time scale is strongly temperature dependent [7,34–38]. Although MCT recognizes the distinction between microscopic and structural relaxation, its main insights deal only with the structural dynamics.

MCT predicts that there is a further division of the structural dynamics into α and β regions, with the β region occurring earlier than the α region,

$$R_{\mathrm{MCT}}(t) \approx \begin{cases} R_\alpha(t), & t \gtrsim \tau_\alpha, \quad R < f \\ R_\beta(t), & t \sim \tau_\beta, \quad R \sim f. \end{cases} \tag{3}$$

These regions are not mutually exclusive and may overlap. They are only defined as regions in which certain approximations to the full response function are valid. The β relaxation of MCT should also be distinguished from the β peaks seen in dielectric relaxation of some liquids [73–75]. More elaborate versions of MCT are needed to deal with β peaks [23,24].

The α region comprises the main relaxation to final equilibrium. MCT predicts simple scaling within the α region, $R_\alpha(t,T) = R_\alpha(t/\tau_\alpha(T))$. In this region, the exact MCT solutions are well approximated by stretched exponentials,

$$R_\alpha(t) = f_c\ \exp\left[-\left(\frac{t}{\tau_\alpha}\right)^{\beta_M}\right]. \tag{4}$$

The scaling relation implies that β_M is constant with temperature. Unlike the standard analysis, the stretched exponential form and the α-scaling properties are expected to be valid only in a region $t > \tau_\alpha$. At sufficiently short times, these relations should fail; however, at these times β-relaxation formulas become valid.

In the β region, the relaxation function is approximated by a more complex form,

$$R_\beta(t) = f_c + \frac{d}{\tau_\beta^a}\, g_\lambda(t/\tau_\beta). \tag{5}$$

This form is expected to hold in a region near τ_β. The function g_λ is a complex function whose shape depends on the value of the exponent parameter λ. Series approximations to numerical solutions of g_λ have been tabulated [76], and these functions have been used in our analysis. Although R_β does not obey a simple scaling law in this region, $g_\lambda \propto \tau_\beta^a (R_\beta - f_c)$ does for $T > T_c$.

The constant f_c is shared by the α and β regions. The temperature dependence of the Debye-Waller factor and, in particular, the well-known prediction of a Debye-Waller cusp at T_c is contained in g_λ. Below T_c, g_λ decays to a constant. The value of this constant, the temperature dependence of τ_β [Eq. (7) below] plus f_c gives the well-known $(T_c - T)^{1/2}$ prediction for the experimental Debye-Waller factor below T_c [22–24]. Above T_c, g_λ has an inflection point at f_c near τ_β. An experimental Debye-Waller factor may be observable at this point, if g_λ is flat enough at the inflection point. The portions of g_λ for $t > \tau_\beta$ contain the von Schweidler limiting law, $g_\lambda \to -t^b$, and the portions for $t < \tau_\beta$ contain the critical limiting law, $g_\lambda \to t^{-a}$. Frequently, the von Schweidler and critical limiting laws hold over such a narrow region that experimental observation of the laws is not expected [76]. The full g_λ function contains higher-order corrections to these limiting laws, and should give better fits to experimental data.

Equations (3)–(5) together define a more complex relaxation function than that given by the standard analysis. Both the average time scale and the shape of $R_{\mathrm{MCT}}(t)$ change with temperature. These changes are determined by the two time constants $\tau_\alpha(T)$ and $\tau_\beta(T)$. MCT makes additional predictions about the temperature dependence of these constants:

$$\tau_\alpha = c_\alpha (T - T_c)^{-\gamma}, \quad T > T_c, \tag{6}$$

$$\tau_\beta = c_\beta |T - T_c|^{-1/2a}. \tag{7}$$

Both time constants diverge at a temperature T_c. Below T_c, the α relaxation is frozen. The β relaxation persists below T_c, becoming faster, but of lower amplitude, as the temperature decreases. The exponents in these power laws are not new independent parameters, but can be calculated from the value of λ used to define the shape of $R_\beta(t)$ in the β region [Eq. (5)] [76]. Because the temperature variations of τ_α and τ_β are different, $R_{\mathrm{MCT}}(t)$ has a temperature-dependent shape

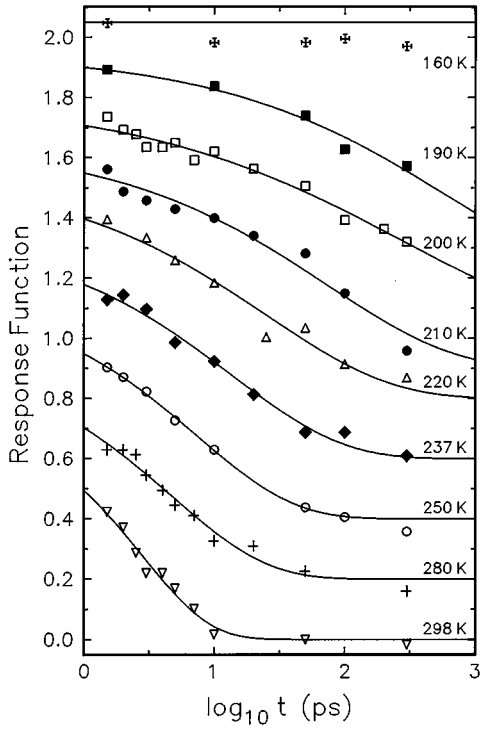

FIG. 2. Solvation response functions for *s*-tetrazine in propylene carbonate fit with stretched exponentials [Eq. (1)]. The β_e parameter of the fits is not constant, violating the time-temperature superposition principle (see Fig. 3). Each temperature has been offset vertically for clarity. (Symbol, offset): (▽, 0), 298 K; (+, 0.2), 280 K; (○, 0.4), 250 K; (♦, 0.6), 237 K; (△, 0.8), 220 K; (●, 0.9), 210 K; (□, 1.05), 200 K; (■, 1.2), 190 K; (✠, 1.3), 160 K. Not shown: 295, 270, 257, and 230 K.

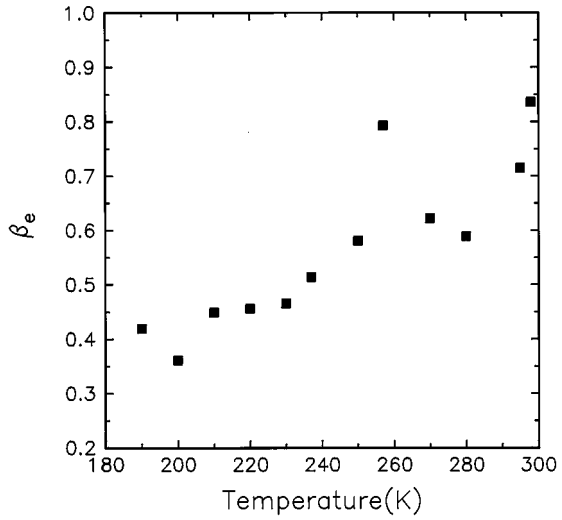

FIG. 3. The temperature dependence of β_e needed to fit stretched exponentials to solvation data in propylene carbonate (see Fig. 2).

and, if examined over a wide range, will not obey the time-temperature superposition principle.

These equations come from the so-called idealized MCT. In the extended version of MCT, the divergences at T_c are rounded, causing the laboratory glass transition to occur at a lower temperature T_g [23,24]. The idealized version of MCT should be valid except for a small temperature region near T_c and for very long times. None of our measurements falls into these regions, so we will only employ the simpler idealized version of MCT.

To fully define the temperature dependence of $R_{\mathrm{MCT}}(t;T)$, MCT requires seven independent parameters: T_c, λ, f_c, β_M, d, c_α, and c_β. Of these, f_c, β_M, d, and c_α depend on the exact dynamical process being measured. Because of these parameters, response functions measured by neutron scattering, light scattering, dielectric relaxation, and transient hole burning are different in detail [33]. However, all experiments should share the same values of T_c and λ, as well the γ and a exponents derived from λ. In some analyses of experimental data, the constants f_c and d are also allowed to have some temperature dependence. We will not do this, but will require that they be strict constants.

III. PROPYLENE CARBONATE

Propylene carbonate is a very fragile glass former with a glass transition temperature $T_g=160$ K [75]. Its dynamics have been studied by neutron [55,59], Brillouin [42,48,52,55] and depolarized light scattering [42] and dielectric relaxation [77–80]. We have measured the solvation response function for propylene carbonate in the temperature range 160–270 K using *s*-tetrazine as the probe solute molecule [33].

A. Standard analysis

The solvation response functions in propylene carbonate are shown in Fig. 2 along with stretched exponential fits [Eq. (1)] [33]. The response functions are absolute measurements, i.e., $R(0)=1$. Phonon dynamics, which are faster than the experimental time resolution, cause the earliest points to be less than 1. The amplitude of the structural component of the dynamics is kept at a constant value of $A=0.75$ in the fitting. Note that an amplitude this large is needed to fit the data at 190 K, but causes a small but significant mismatch at 160 K, near the glass transition.

Although stretched exponentials can be fit to the response functions, the time-temperature superposition is strongly violated. As the $1/e$ time becomes longer at lower temperatures, some relaxation remains even at the earliest times. Increased stretching (smaller β_e) is required as the temperature is lowered. The temperature dependence of β_e needed in the fits is shown in Fig. 3. Once β_e is allowed to vary with temperature, the number of adjustable parameters in the fit is significantly increased, and the appealing simplicity of the standard analysis is reduced.

If this problem is ignored, the average relaxation times extracted from the fits can be fit to a Vogel-Fulcher form [Eq. (2)] as shown in Fig. 4. Although the Vogel-Fulcher form is satisfied for the solvation data to within experimental accuracy, viscosity data show that it is not generally satisfactory [81]. Values in the range of $T_0=122$–150 K and

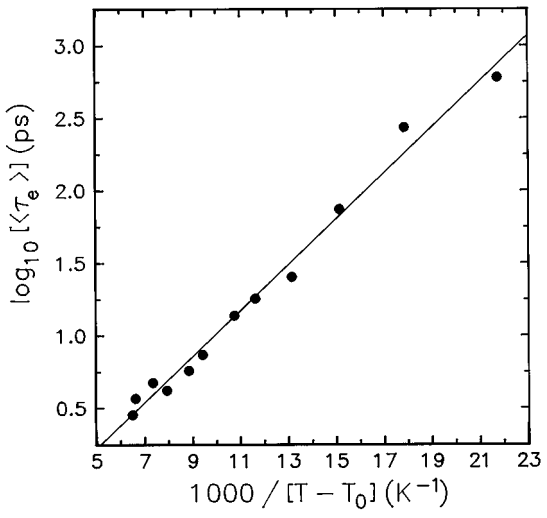

FIG. 4. A Vogel-Fulcher plot of the average relaxation times from a standard analysis of propylene carbonate solvation [Eq. (2), τ_e^0=270 fs, T_0=144 K, D=2.53].

D=1.27–5.47 are found depending on the temperature range fit.

B. Mode-coupling analysis

The results of a mode-coupling fit to the propylene carbonate data are shown in Figs. 5–8. Figure 5 shows the scaling behavior expected in the α region. The data from each temperature have been shifted in time until the lower portions of the response functions match. The behavior of the upper portion of the response functions is not considered in the fitting, because this region will be shown later to contain β relaxation. The time shifts needed for scaling yield τ_α's. A stretched exponential [Eq. (4)] is fit to the α region with β_M=0.8 and f_c=0.56. The predicted time-temperature scaling relationship is found within the α region.

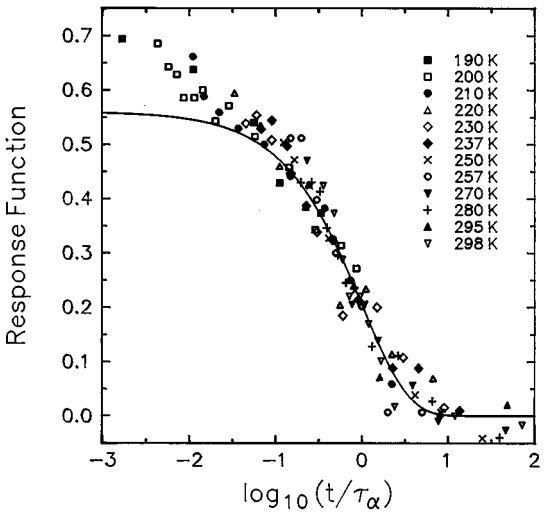

FIG. 5. An α-scaling plot for propylene carbonate along with a stretched exponential representing $R_\alpha(t/\tau_\alpha)$ [Eq. (4), f_c=0.65, β_M=0.8]. The deviations at short times are attributed to β relaxation.

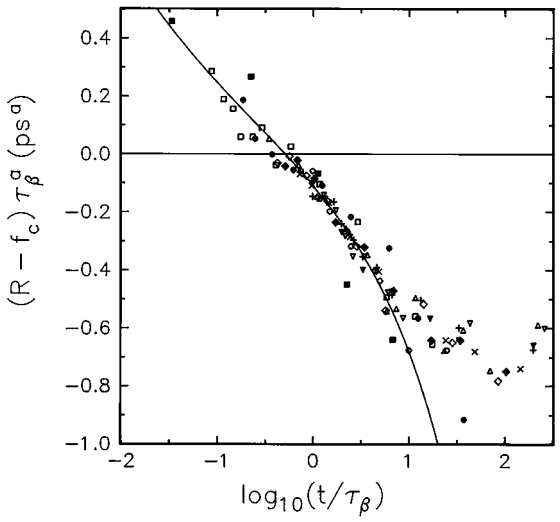

FIG. 6. A β-scaling plot for propylene carbonate along with the scaling function $g_\lambda(t/\tau_\beta)$ [Eq. (5), λ=0.78, f_c=0.56]. The deviations at long times are attributed to α relaxation. See Fig. 5 for symbols.

For the region with $R>0.5$, there are strong deviations from R_α. A close examination of the data below 220 K in Fig. 5 shows that the deviations occur earlier in scaled time as the temperature is lowered, and the data do not appear to be approaching a short-time asymptote. This behavior is expected for β relaxation.

Figure 6 shows that the upper portions of the response function do indeed fit the scaling relation expected for β relaxation [Eq. (5)]. The scaling is done with the same value of f_c=0.56 used in fitting the α relaxation. The exponent parameter λ=0.78 found from light-scattering data [42] is also used here. The value of λ fixes the shape of $g_\lambda(t/\tau_\beta)$, which is shown along with the data. The exponent a=0.29

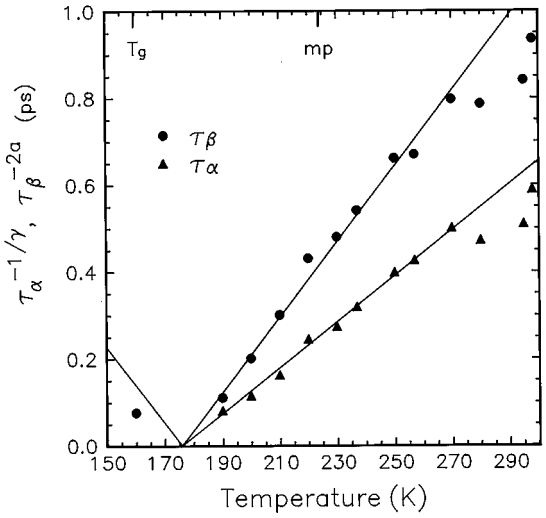

FIG. 7. Power-law fits to the MCT scaling times [Eqs. (6) and (7)] from propylene carbonate. A value of T_c=176 K is found. The exponents (α=0.29, γ=2.706) are determined by the value of λ used in the scaling analysis. The fit lines (c_α=1.45×10^6 ps K$^\gamma$, c_β=3.58×10^3 ps K$^{1/2\alpha}$) are constrained to have the same x intercept, i.e., the same T_c.

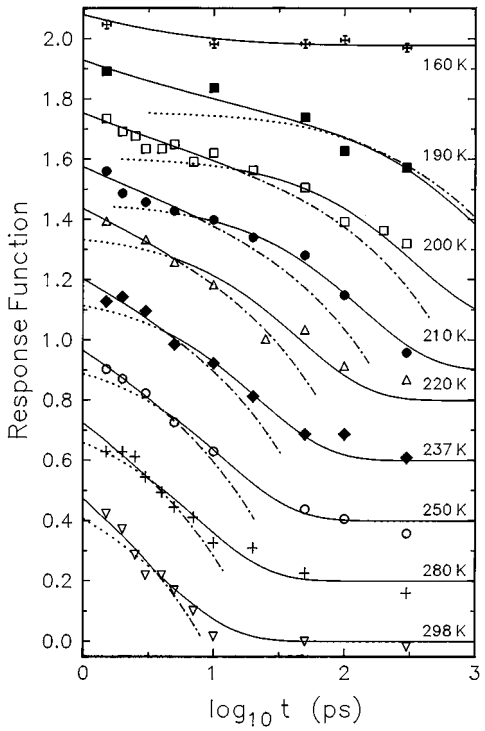

FIG. 8. Solvation response functions in propylene carbonate along with the fits from mode-coupling theory (Figs. 5 and 6). The solid lines are a combination of R_α at long times and R_β at short times, joined at their crossing point. Only R_β is shown at 160 K. The continuations of R_α (dotted) and R_β (dot-dashed) beyond the crossing point are also shown. The α and β regions overlap strongly, and a well-defined Debye-Waller factor is not formed in this temperature region. Each temperature has been offset vertically for clarity. See Fig. 2 for symbols and offsets.

used in the scaling is also fixed by the value of λ [76]. Only the time τ_β is adjusted to scale the data. The predicted scaling is found at short and intermediate times. As expected, the data deviate from the β-relaxation function at times sufficiently longer than τ_β. In the long-time regime, the data are accounted for by the α-relaxation function (Fig. 5).

One temperature point at 160 K cannot be included on the scaling plot in Fig. 6. It is near the glass transition temperature T_g and definitely below T_c, where g_λ changes its form. However, a fit to Eq. (5) with the same parameters can still be made, and is shown in Fig. 8. A weak, but rapid, β decay to a constant is expected in this temperature region. Although the amplitude of the decay is near the experimental precision, the decay time, amplitude, and the long-time asymptote are simultaneously fit by adjusting the single parameter τ_β.

The α- and β-scaling fits presented above were found by an iterative procedure. Three parameters aside from the scaling times were needed, d, β_M, and f_c. Because f_c is shared by the α- and β-scaling relations, fitting one region affects the other. Fits of α scaling to the lower portion of $R(t)$ were alternated with β-scaling fits to the middle section of $R(t)$. There are reasonably sharp limits to the time ranges that can be fit with each formula, regardless of the parameters used. Thus there is only a small amount of uncertainty in the fit parameters resulting from the choice of time ranges fit.

The scaling fits produce two time constants, τ_α and τ_β, for each temperature. These time constants should fit the power-law temperature dependencies given by Eqs. (6) and (7). The exponents a and γ are fixed by the choice of λ above [76]. The value of T_c must also be the same for both the α and β times. Fits under these conditions are shown in Fig. 7. Good fits are found for temperatures as high as 270 K. The increased mismatch above 270 K may be due to the expected failure of MCT at sufficiently high temperatures. On the other hand, the time scales for relaxation at these temperatures are short enough that the dynamic range of the data is reduced, which may cause additional experimental error. Thus we are not confident that MCT has failed, even above 270 K.

At this point we can make a specific comparison of the parameters λ and T_c obtained here and by light scattering [42]. In fitting the solvation data, there is some interdependence in the values of λ and T_c. Using the value of $\lambda=0.78$ found by light scattering gives fits within the best-fit range. In the reported results, λ has been fixed at 0.78, and T_c has been fit entirely independently of the light-scattering results. The solvation value of $T_c=176$ K is close to the light-scattering value $T_c=179\pm2$ K (from the extended MCT analysis) [42].

The light-scattering experiments required an extended MCT analysis, because measurements close to T_c were available. That analysis indicated that the crossover region, where deviations from ideal MCTs are expected, is approximately 10 K wide [42]. Because none of the solvation measurements falls within this range, the ideal MCT treatment used here is expected to be sufficient.

An important conclusion from the MCT fitting is best illustrated by plotting the R_α and R_β MCT functions against the data in real time (Fig. 8). The complete response function R_{MCT} is approximated by simply joining the short-time portion of R_β to the long-time portion of R_α at their crossing point. The α- and β-scaling regions overlap heavily over most of the temperature range. A clear plateau region at f_c is not seen. The analysis of Debye-Waller factors to test MCT requires a clear time-scale separation between α and β regions. For propylene carbonate, such a test will fail at temperatures slightly above T_c, whereas an analysis of response functions as given here still finds agreement with MCT predictions.

IV. *n*-BUTYLBENZENE

n-butylbenzene is another fragile glass former with a glass transition temperature $T_g=128$ K. The solvation response function for *n*-butylbenzene has been measured at 165–240 K using dimethyl-*s*-tetrazine as the probe solute molecule [34].

A. Standard analysis

In contrast to propylene carbonate, a standard analysis of *n*-butylbenzene solvation dynamics is straightforward and quite successful. Figure 9 shows the solvation data with stretched exponential [Eq. (1)] fits. Both the amplitude A and shape parameter β_e are constant with temperature. The time-temperature superposition principle holds within a small error. Figure 10 reinforces this conclusion with a master plot of

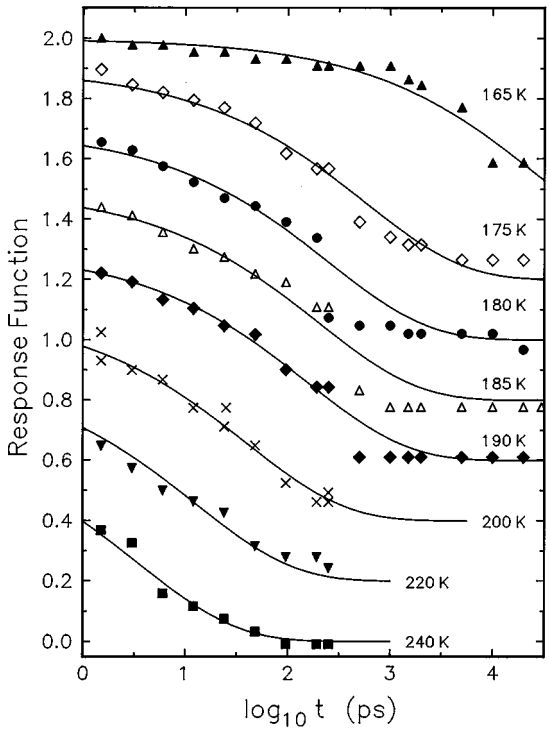

FIG. 9. Solvation response functions for dimethyl-*s*-tetrazine in *n*-butylbenzene fit with stretched exponentials [Eq. (1)]. The β_e parameter of the fits is constant, in conformity with the time-temperature superposition principle (see Fig. 10). Each temperature has been offset vertically for clarity. (Symbol, offset): (■, 0), 240 K; (▼, 0.2), 220 K; (*X*, 0.4), 200 K; (◆, 0.6), 190 K; (△, 0.8), 185 K; (●, 1.0), 180 K; (◇, 1.2), 175 K; (▲, 1.3), 165 K. Not shown: 250, 230, 210, and 195 K.

the data. The temperature dependence of the relaxation times obtained from the master plot can be fit to a Vogel-Fulcher form [Eq. (2), Fig. 11].

Despite the general success of the standard treatment, there are small discrepancies at short times and low temperatures, just as there were in propylene carbonate. These are most noticeable in Fig. 10 for 165 and 175 K. The slope of the data does not seem to be decreasing to zero at short times as it should.

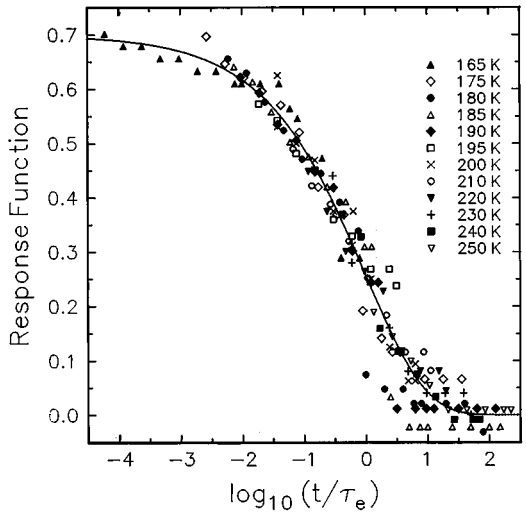

FIG. 10. A master plot of *n*-butylbenzene solvation data along with a stretched exponential fit [Eq. (1), $A=0.7$, $\beta_e=0.45$].

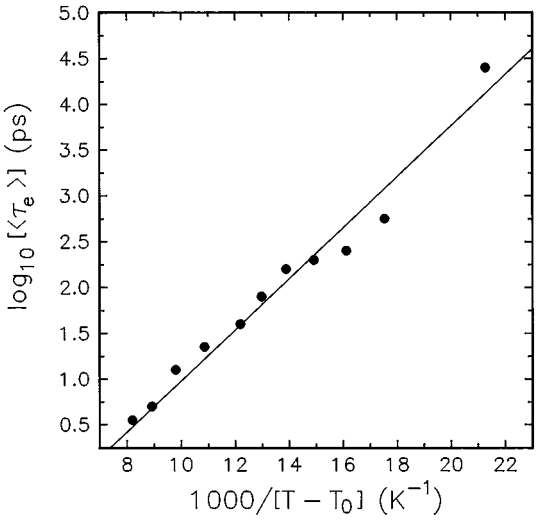

FIG. 11. A Vogel-Fulcher plot of the average relaxation times from a standard analysis of *n*-butylbenzene solvation [Eq. (2), $\tau_e^0=15.5$ fs, $T_0=118$ K, $D=5.44$].

B. Mode-coupling analysis

Although the standard analysis of the *n*-butylbenzene data is satisfactory, we must ask if a MCT analysis works equally well. At first, it might seem that a MCT fit is obtained trivially by letting $\tau_\alpha=\tau_e$ and $f_c=A$. However, such a fit is not consistent with the predictions of MCT regarding β relaxation. As $R_{\mathrm{MCT}}(t)$ approaches f_c at short times, the β-scaling law [Eq. (5)] must be followed. This scaling is incompatible with the α-scaling law [Eq. (4)] at longer times. Thus MCT predicts that the time-temperature superposition principle must fail at short times, and the success of the master plot in

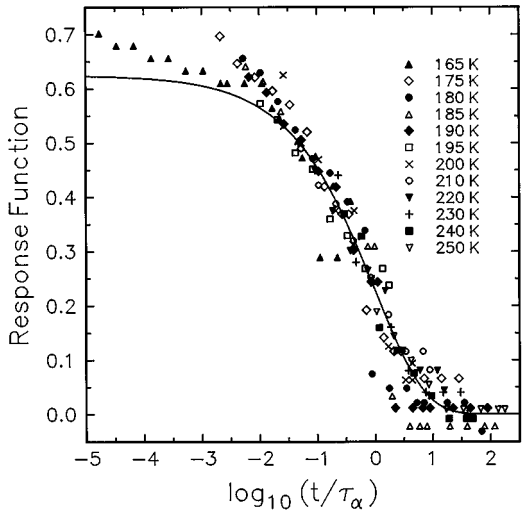

FIG. 12. An α-scaling plot for *n*-butylbenzene along with a stretched exponential representing $R_\alpha(t/\tau_\alpha)$ [Eq. (4), $f_c=0.625$, $\beta_M=0.5$]. The deviations at short times are attributed to β relaxation.

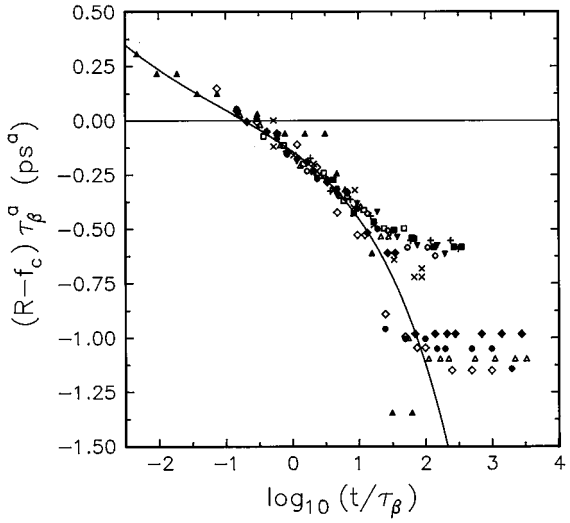

FIG. 13. A β-scaling plot for *n*-butylbenzene along with the scaling function $g_\lambda(t/\tau_\beta)$ [Eq. (5), $\lambda=0.86$, $f_c=0.625$]. The deviations at long times are attributed to α relaxation. See Fig. 12 for symbols.

Fig. 10 would seem to prove the MCT wrong. However, we will show that a MCT fit, including a violation of the time-temperature superposition principle at short times, fits the experimental data as well or better than the standard analysis.

Because separate α and β regions are not readily apparent in the raw data, an iterative fitting procedure was used consisting of the following steps: (1) A value of f_c was estimated from the short-time, low-temperature data. An α-scaling analysis was performed on data below 0.8 f_c. A value of β_M and a set of τ_α's resulted. The temperature dependence of the τ_α's could satisfy Eq. (6) for a range of (λ, T_c^α) values. (2) For each (λ, T_c^α) pair, a set of β-scaling times was found from Eq. (7). In a plot of R vs t/τ_β, the data

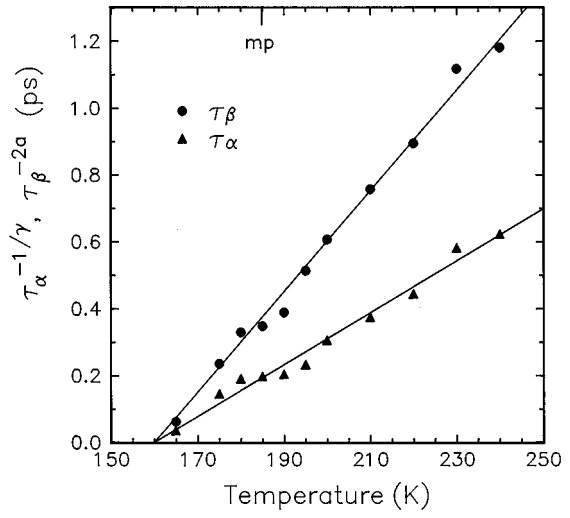

FIG. 14. Power-law fits to the MCT scaling times [Eqs. (6) and (7)] from *n*-butylbenzene. A value of $T_c=160$ K is found. The exponents ($\alpha=0.241$, $\gamma=3.408$) are determined by the value of λ used in the scaling analysis. The fit lines ($c_\alpha=1.55\times10^7$ ps K$^\gamma$, $c_\beta=6.03\times10^3$ ps K$^{1/2a}$) are constrained to have the same x intercept, i.e., the same T_c.

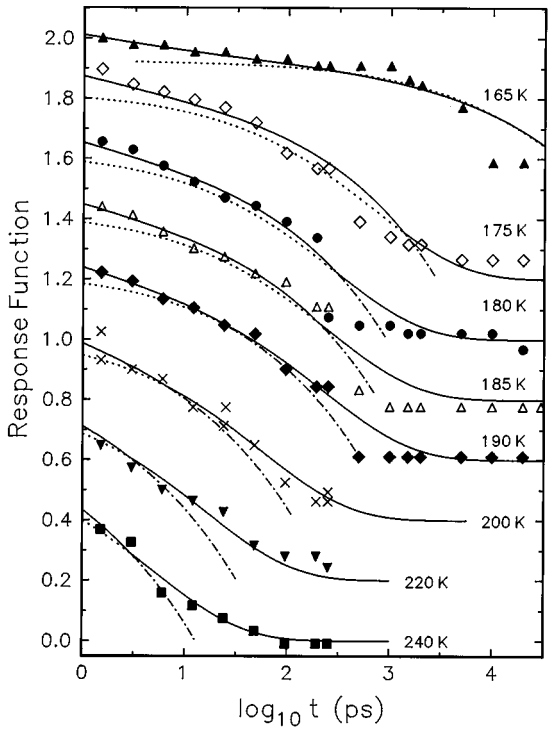

FIG. 15. Solvation response functions in *n*-butylbenzene along with the fits from mode-coupling theory (Figs. 12 and 13). The solid lines are a combination of R_α at long times and R_β at short times, joined at their crossing point. The continuations of R_α (dotted) and R_β (dot-dashed) beyond the crossing point are also shown. Each temperature has been offset vertically for clarity. See Fig. 9 for symbols and offsets.

cross at a point that gave a revised value of f_c. (3) For a range of λ's, a β-scaling analysis was performed with the f_c found in step (2). The fitting ignored the small values of $R(t)$ at long times. A value of d and a set of τ_β's resulted. The temperature dependence of the τ_β's defined a T_c^β for each value of λ. Fitting to Eq. (5) further refined f_c. (4) With the new value of f_c, steps (1)–(3) were repeated until an optimum set of parameters was found.

For the desired value of λ, the α and β regions are consistent with each other, $T_c^\alpha(\lambda)=T_c^\beta(\lambda)$. This occurred in a region $\lambda=0.86$–0.84 and $T_c=159$–161 K. Self-consistent fits were not found near $T_c=150$ K, the value reported by ISTS experiments [39].

The results of the fitting are shown in Figs. 12–14. The α-scaling plot in Fig. 12 is very similar to the master plot (Fig. 10) in the standard analysis, except the stretched exponential portion of the response function is confined to the lower portion of the response. The deviations from the α fit at short scaled times are attributed to β relaxation. As expected, the deviations occur earlier in scaled time as the temperature is raised.

Figure 13 shows that this early behavior can indeed be explained as β relaxation. The β-scaling plot accounts for the data near τ_β. It only fails at long times, where the α-scaling relations are adequate. Comparing Figs. 13 and 10, the MCT analysis gives a better account of the short-time data at 165 and 175 K than the standard analysis.

The consistency of the α and β scaling is demonstrated in Fig. 14. The power-law temperature dependencies of τ_α and τ_β [Eqs. (6) and (7)] hold with a common value of T_c. The exponents for the power laws, a and γ, are derived from the exponent parameter λ used in fitting the β-relaxation region.

Figure 15 shows the solvation data along with R_α and R_β in real time. The overlap of the ranges of validity of these two approximations is even greater than in propylene carbonate.

V. DISCUSSION

The first criterion for assessing MCT must be its ability to correctly describe the experimental data. In both liquids examined, MCT provides a consistent description of both the temperature-dependent changes in time scale and the shape of the solvation response function. There was no need to introduce temperature dependence to the constants of the theory.

A more subtle question is whether MCT or the standard analysis provide a better description of the data on a purely empirical basis. The most important difference in the treatments is the prediction of a β-relaxation region by MCT. In the case of propylene carbonate, the standard analysis can only be applied if β_e is made temperature dependent, causing a significant increase in the number of fitting parameters. In the MCT fits, the β-relaxation component explains the strongly temperature-dependent relaxation shape without compromising the model. Thus, MCT is superior on a purely empirical basis.

In *n*-butylbenzene, the standard analysis is nearly as good in fitting the data as the MCT, although MCT is slightly better at describing the data at the lowest temperatures and shortest times. Although the differences are near the level of experimental error, the improvement is in exactly the region where the effects of β relaxation are expected to be greatest.

In the MCT analysis, the β relaxation is still present in *n*-butylbenzene, but is less evident, because τ_α and τ_β are too close to each other for a clear plateau region to form. The dangers of assuming that α and β regions are always separated and can be analyzed independently has been pointed out before [42,45,76] and is clearly illustrated by this example.

This example also shows that many experiments, which have previously been analyzed by standard methods and do not have obvious β-relaxation features, may be amenable to reinterpretation according to MCT. In particular, β relaxation has not been previously identified in solvation experiments, even those focusing on the supercooled region [28–38]. However, complex and temperature-dependent relaxation functions are commonly seen. Mode-coupling theory offers a potentially fruitful approach to understanding those results.

The current approach to MCT data fitting, along with most other experimental analyses, focuses on general scaling relations. This approach has a weakness, which is illustrated in Figs. 8 and 15. Although the α and β regions are fit well on scaling plots and share the parameters f_c, λ, and T_c, the results from the two regions are not completely consistent. Figures 8 and 15 show that when complete $R(t)$ functions are examined, there are noticeable discontinuities in the slopes at the points joining the α and β regions. Greater efforts to construct complete MCT response functions will provide a more rigorous test of MCT [56].

Beyond fitting the data from a specific experiment, an important test of MCT is the transferability of T_c and λ among different experiments on the same liquid. Such transferability indicates that these parameters have genuine physical significance and are not arbitrary fitting parameters. In the case of propylene carbonate, good agreement exists between solvation and light scattering [42]. The actual relaxation times found by light scattering and solvation are numerically different and have a different temperature dependence (Ref. [33], Fig. 9). Thus the ability of MCT to identify a connection between these experiments is not trivial and is a strong point in favor of MCT.

Comparison of neutron and light-scattering results on $Ca_{0.4}K_{0.6}(NO_3)_{1.4}$ has shown a greater degree of transferability than found here [51,56]. In our notation, c_β was also found to transfer between the experiments. Fitting Du *et al.*'s light-scattering results on propylene carbonate [42] to Eq. (7) gives $c_\beta = 1.00\times10^3$ ps $K^{1/2a}$. This value is substantially smaller than the value found in solvation, $c_\beta = 3.58\times10^3$ ps $K^{1/2a}$.

For *n*-butylbenzene, the case is less clear. Recent ISTS experiments have identified $T_c = 150$ K from a cusp in the Debye-Waller factor [39]. This value is 10 K lower than the value obtained in this paper. Although the difference is not big, it is larger than can be accommodated by the experimental error ranges. Unfortunately, the temperature ranges of the two experiments do not overlap. Requiring that MCT simultaneously account for data both above and below T_c is more demanding and may result in some inconsistency between the two analyses. Also, the hopping effects predicted by extended MCTs complicate the region near T_c and have not been taken into account in either experimental analyses. Further attempts to resolve these two experiments are merited.

Mode-coupling theory is generally associated with supercooled liquids and the glass transition. It is explicitly developed as an expansion about a temperature T_c at which the liquid has a moderately high viscosity. On the other hand, much of the current work in solvation dynamics is focused on liquids above their melting points, where the viscosity is low and relaxation times are a few picoseconds or less. Mode-coupling theory might not seem relevant to these experiments; however, we have not been able to reliably find the point where MCT breaks down as the temperature is raised. The MCT relations hold to at least 270 K in propylene carbonate (melting point of 224 K) and 240 K in *n*-butylbenzene (melting point of 185 K). At these points, the viscosities are down to 3.4 and 4.8 cP and the τ_β's are as short as 1.5 and 0.7 ps in propylene carbonate and *n*-butylbenzene, respectively. The validity of MCT at high temperatures, the role of β relaxation at low viscosities, and the interaction of β relaxation and microscopic motion as τ_β becomes smaller are questions that have not been carefully explored yet, but may have important implications in understanding dynamics in the normal as well as supercooled regions.

ACKNOWLEDGMENTS

We thank Professor W. Götze for insightful comments on the manuscript. This paper is based upon work supported by the National Science Foundation.

[1] M. Maroncelli, J. Mol. Liq. **57**, 1 (1993).
[2] P. F. Barbara and W. Jarzeba, Adv. Photochem. **15**, 1 (1990).
[3] B. Bagchi, Annu. Rev. Phys. Chem. **40**, 115 (1989).
[4] E. W. Castner, Jr., B. Bagchi, M. Maroncelli, S. P. Webb, A. J. Ruggiero, and G. R. Fleming, Ber. Bunsenges. Phys. Chem. **92**, 363 (1988).
[5] J. G. Saven and J. L. Skinner, J. Chem. Phys. **99**, 4391 (1993).
[6] B. Bagchi, J. Chem. Phys. **100**, 6658 (1994).
[7] M. Berg, Chem. Phys. Lett. **228**, 317 (1994).
[8] R. M. Stratt and M. Cho, J. Chem. Phys. **100**, 6700 (1994).
[9] B. M. Ladanyi and R. M. Stratt, J. Phys. Chem. **99**, 2502 (1995).
[10] B. M. Ladanyi and R. M. Stratt, J. Phys. Chem. **100**, 1266 (1996).
[11] R. Jimenez, G. R. Fleming, P. V. Kumar, and M. Maroncelli, Nature **369**, 471 (1994).
[12] M. L. Horng, J. Gardecki, A. Papazyan, and M. Maroncelli, J. Phys. Chem. **99**, 17 311 (1995).
[13] L. Reynolds, J. A. Gardecki, S. J. V. Frankland, M. L. Horng, and M. Maroncelli, J. Phys. Chem., **100**, 10 337 (1996).
[14] J.-Y. Bigot, M. Portella, R. W. Schoenlein, C. J. Bardeen, A. Migus, and C. V. Shank, Phys. Rev. Lett. **66**, 1138 (1991).
[15] C. J. Bardeen and C. V. Shank, Chem. Phys. Lett. **266**, 310 (1994).
[16] E. T. J. Nibbering, D. A. Wiersma, and K. Duppen, Phys. Rev. Lett. **68**, 514 (1992).
[17] K. Duppen, F. de Haan, E. T. J. Nibbering, and D. A. Wiersma, Phys. Rev. A **47**, 5120 (1993).
[18] M. Cho and G. R. Fleming, J. Chem. Phys. **98**, 2848 (1993).
[19] M. Cho and G. R. Fleming, J. Phys. Chem. **98**, 3478 (1994).
[20] T. Joo, Y. Jia, and G. R. Fleming, J. Chem. Phys. **102**, 4063 (1995).
[21] P. Vöhringer, D. C. Arnett, R. A. Westervelt, M. J. Feldstein, and N. F. Scherer, J. Chem. Phys. **102**, 4027 (1995).
[22] R. Schilling, in *Disorder Effects on Relaxational Processes: Glasses, Polymers, Proteins*, edited by R. Richert and A. Blumen (Springer-Verlag, New York, 1994).
[23] W. Götze and L. Sjögren, Rep. Prog. Phys. **55**, 241 (1992).
[24] W. Götze, in *Liquids, Freezing and Glass Transition*, edited by J. P. Hansen, D. Levesque, and J. Zinn-Justin (North-Holland, Amsterdam, 1991).
[25] H. Z. Cummins, G. Li, W. M. Du, and J. Hernandez, Physica A **204**, 169 (1994).
[26] W. Götze and L. Sjögren, Trans. Theory Stat. Phys. **24**, 801 (1995).
[27] W. Götze and L. Sjögren, Chem. Phys. (to be published).
[28] R. Richert, F. Stickel, R. S. Fee, and M. Maroncelli, Chem. Phys. Lett. **229**, 302 (1994).
[29] R. Richert, Chem. Phys. Lett. **216**, 223 (1993).
[30] R. Richert, Chem. Phys. Lett. **199**, 355 (1992).
[31] R. Richert and A. Wagener, J. Phys. Chem. **95**, 10 115 (1991).
[32] R. Richert, Chem. Phys. Lett. **171**, 222 (1990).
[33] J. Ma, D. Van den Bout, and M. Berg, J. Chem. Phys. **103**, 9146 (1995).
[34] J. T. Fourkas and M. Berg, J. Chem. Phys. **98**, 7773 (1993).
[35] J. T. Fourkas, A. Benigno, and M. Berg, J. Chem. Phys. **99**, 8552 (1993).
[36] J. Yu and M. Berg, J. Phys. Chem. **97**, 1758 (1993).
[37] J. Yu and M. Berg, J. Chem. Phys. **96**, 8741 (1992).
[38] J. Yu, P. Earvolino, and M. Berg, J. Chem. Phys. **96**, 8750 (1992).
[39] Y. Yang, L. J. Muller, and K. A. Nelson (unpublished).
[40] Y. Yang and K. A. Nelson, J. Chem. Phys. **103**, 7732 (1995); Phys. Rev. Lett. **74**, 4883 (1995).
[41] M. J. Lebon, C. Dreyfus, G. Li, A. Aouadi, H. Z. Cummins, and R. M. Pick, Phys. Rev. E **51**, 4537 (1995).
[42] W. M. Du, G. Li, H. Z. Cummins, M. Fuchs, J. Toulouse, and L. A. Knauss, Phys. Rev. E **49**, 2192 (1994).
[43] W. Steffen, A. Patkowski, H. Gläser, G. Meier, and E. W. Fischer, Phys. Rev. E **49**, 2992 (1994).
[44] E. Rössler, A. P. Sokolov, A. Kisliuk, and D. Quitmann, Phys. Rev. B **49**, 14 967 (1994).
[45] G. Li, W. M. Du, J. Hernandez, and H. Z. Cummins, Phys. Rev. E **48**, 1192 (1993).
[46] H. Z. Cummins, W. M. Du, M. Fuchs, W. Götze, S. Hildegrand, A. Latz, G. Li, and N. J. Tao, Phys. Rev. E **47**, 4223 (1993).
[47] I. C. Halalay and K. A. Nelson, J. Chem. Phys. **97**, 3557 (1992).
[48] M. Elmroth, L. Börjesson, and L. M. Torell, Phys. Rev. Lett. **68**, 79 (1992).
[49] C. Dreyfus, M. J. Lebon, H. Z. Cummins, J. Toulouse, B. Bonello, and R. M. Pick, Phys. Rev. Lett. **69**, 3666 (1992).
[50] G. Li, W. M. Du, A. Sakai, and H. Z. Cummins, Phys. Rev. A **46**, 3343 (1992).
[51] G. Li, W. M. Du, X. K. Chen, H. Z. Cummins, and N. J. Tao, Phys. Rev. A **45**, 3867 (1992).
[52] L. Börjesson, M. Elmroth, and L. M. Torell, J. Non-Cryst. Solids **131–133**, 139 (1991).
[53] M. Fuchs, W. Götze, and A. Latz, Chem. Phys. **149**, 185 (1990).
[54] J. Wuttke, J. Hernandez, G. Li, G. Coddens, H. Z. Cummins, F. Fujara, W. Petry, and H. Sillescu, Phys. Rev. Lett. **72**, 3052 (1994).
[55] L. Börjesson, M. Elmroth, and L. M. Torell, Chem. Phys. **149**, 209 (1990).
[56] M. Fuchs and H. Z. Cummins, Philos. Mag. B **71**, 771 (1995).
[57] Ch. Simon, G. Faivre, R. Zorn, F. Batallan, and J. F. Legrand, J. Phys. (France) I **2**, 307 (1992).
[58] M. Kiebel, E. Bartsch, O. Debus, F. Fujara, W. Petry, and H. Sillescu, Phys. Rev. B **45**, 10 301 (1992).
[59] L. Börjesson and W. S. Howells, J. Non-Cryst. Solids **131–133**, 53 (1991).
[60] W. Petry, E. Bartsch, F. Fujara, M. Keibel, H. Sillescu, and B. Farago, Z. Phys. B **83**, 175 (1991).
[61] F. Mezei, J. Non-Cryst. Solids **131–133**, 317 (1991).
[62] B. Frick, B. Farago, and D. Richter, Phys. Rev. Lett. **64**, 2921 (1990).
[63] E. Bartsch, F. Fujara, M. Kiebel, H. Sillescu, and W. Petry, Ber. Bunsenges. Phys. Chem. **93**, 1252 (1989).
[64] S. Jung, P. Müller, and C. Morkel, in *Hydrogen Bonded Liquids*, edited by J. C. Dore and José Teixeira, Springer Proceedings in Physics Vol. 37 (Kluwer Academic, Boston, 1989).
[65] D. Richter, B. Frick, and B. Farago, Phys. Rev. Lett. **61**, 2465 (1988).
[66] W. Knaak, F. Mezei, and B. Farago, Europhys. Lett. **7**, 529 (1988).
[67] B. Frick, D. Richter, W. Petry, and U. Buchenau, Z. Phys. B. **70**, 73 (1988).
[68] F. Fujara and W. Petry, Europhys. Lett. **4**, 921 (1987).
[69] U. Krieger and J. Bosse, Phys. Rev. Lett. **59**, 1601 (1987).

[70] F. Mezei, W. Knaak, and B. Farago, Phys. Rev. Lett. **58**, 571 (1987).
[71] *Disorder Effects on Relaxational Processes: Glasses, Polymers, Proteins*, edited by R. Richert and A. Blumen (Springer-Verlag, New York, 1994).
[72] C. P. Lindsey and G. D. Patterson, J. Chem. Phys. **73**, 3348 (1980).
[73] L. Wu, Phys. Rev. B **43**, 9906 (1991).
[74] G. P. Johari and M. Goldstein, J. Chem. Phys. **55**, 4245 (1971).
[75] G. P. Johari and M. Goldstein, J. Chem. Phys. **53**, 2372 (1970).
[76] W. Götze, J. Phys. Condens. Matter **2**, 8485 (1990).
[77] A. Schönhals, F. Kremer, A. Hofmann, E. W. Fischer, and E. Schlosser, Phys. Rev. Lett. **70**, 3459 (1993).
[78] J. Barthel, K. Bachhuber, R. Buchner, J. B. Gill, and M. Kleebauer, Chem. Phys. Lett. **167**, 62 (1990).
[79] R. Payne and I. E. Theodorou, J. Phys. Chem. **76**, 2892 (1972).
[80] E. A. S. Cavell, J. Chem. Soc. Faraday Trans. 2 **70**, 78 (1974).
[81] A. Bondeau and J. Huck, J. Phys. (Paris) **46**, 1717 (1985).